Relativistic and correlated calculations on the ground, excited, and ionized states of iodine

de Jong, W. A.; Visscher, L.; Nieuwpoort, W. C.

Published in:
Journal of Chemical Physics

DOI:
10.1063/1.475194

Relativistic and correlated calculations on the ground, excited, and ionized states of iodine

W. A. de Jong, L. Visscher, and W. C. Nieuwpoort

Citation: J. Chem. Phys. **107**, 9046 (1997); doi: 10.1063/1.475194
View online: https://doi.org/10.1063/1.475194
View Table of Contents: http://aip.scitation.org/toc/jcp/107/21
Published by the American Institute of Physics

Relativistic and correlated calculations on the ground, excited, and ionized states of iodine

W. A. de Jong, L. Visscher,[a] and W. C. Nieuwpoort
Laboratory for Chemical Physics and Materials Science Centre, University of Groningen, Nijenborgh 4, 9747 AG Groningen, The Netherlands

(Received 26 December 1996; accepted 28 August 1997)

The electronic structure, spectroscopic, and bonding properties of the ground, excited, and ionized states of iodine are studied within a four-component relativistic framework using the MOLFDIR program package. The experimentally determined properties of the $^1\Sigma_g^+$ ground state are well reproduced by our results calculated at the CCSD(T) level of theory. Relativistic effects and core–valence correlation need to be included in order to get reliable results, but the Gaunt interaction can be neglected. The photoelectron spectrum and the potential energy curves of the ionized and excited states are calculated using relativistic configuration interaction and coupled cluster methods. The calculated properties of the excited states are generally in good agreement with the experimental data, as well as with the earlier theoretical results of Teichteil and Pelissier. An alternative assignment of some recently measured, low lying, ionized states is proposed. © *1997 American Institute of Physics.* [S0021-9606(97)02945-0]

I. INTRODUCTION

The spectroscopic properties of the iodine molecule have been the subject of many experiments[1–29] and theoretical studies,[30–44] yet our understanding of these properties is still incomplete. Crucial in the understanding of these properties is the effect of relativity. In particular, the spin–orbit interaction, which leads to severe mixing of excited states, has profound implications for the interpretation of spectroscopic data.

The most studied excited state is the $B\ ^3\Pi_u(0_u^+)$, responsible for the visible absorption spectrum, a state that dissociates into $^2P_{3/2}+{}^2P_{1/2}$ atomic states and thereby crosses repulsive or very weakly bound states originating from $^2P_{3/2}+{}^2P_{3/2}$ atomic states. These crossings give rise to a number of predissociation effects that have been observed. Predissociation of the B state is now more or less understood.[4,5,38] Other excited states are, however, much less well characterized. Early theoretical work was done by Mulliken,[30] who constructed a theoretical spectrum based on one-electron arguments and empirical corrections. Tellinghuisen[8–10,12] constructed potential energy curves on the basis of experimental data. State-of-the-art theoretical calculations can nowadays be used to confirm the form and positions of the proposed curves.

Most of the theoretical work is done on the molecular ground state. The majority of the calculations are valence electron calculations, where the core is represented by a relativistic pseudopotential.[31,32,34–36,41] To improve the calculated spectroscopic properties core–valence correlation effects can be included in the pseudopotentials. Another type of calculation applied to the iodine molecule[37] is the Zeroth-Order Regular Approximation (ZORA)[45] method, used in combination with density functional theory.

Some calculations were performed on the excited states of the iodine molecule. All these calculations make use of relativistic pseudopotentials. Das and Wahl[35] have determined a few excited states using the MCSCF method with empirical corrections for the relativistic effects. Li and Balasubramanian[41] and Teichteil and Pelissier[31] calculated the excited states by a MCSCF method followed by spin–orbit (SO) CI calculations. The curves obtained by Li and Balasubramanian differ from those calculated by Teichteil and Pelissier, leading to two different theoretical pictures for the assignment of the I_2 spectra and the interpretation of spectroscopic phenomena like predissociation.

For the ionized states of iodine there is only a limited amount of experimental[20–24,28] and theoretical data available.[41,42] Li and Balasubramanian[41] calculated potential energy curves and spectroscopic properties for the ionized states of iodine. Given the discrepancies between their work and that of Teichteil and Pelissier for the excited states of the neutral molecule, and in the light of the recent ZEKE experiments on the ionized states,[28] another theoretical investigation is of interest.

In this paper the influence of relativity and correlation, including core–valence correlation effects, on the spectroscopic properties of the ground state are studied using the all-electron Dirac–Fock method followed by CCSD(T) calculations. All relativistic effects are hence included from the outset.

The potential energy curves for all excited states that dissociate into the $^2P_J+{}^2P_J$ ($J=3/2$ or $1/2$) atomic states are calculated using the average of configurations Dirac–Hartree–Fock approach,[46] followed by a complete active space CI calculation. This approach allows us to assess the influence of spin–orbit coupling on the spectroscopic properties and makes it possible to assign the observed states. In order to obtain information about the accuracy of the calculated spectra additional MRCISD calculations are performed.

[a]Permanent address: Odense University, Campusvej 55, DK-5230 Odense M, Denmark.

 0021-9606/97/107(21)/9046/13/$10.00

Four low lying states of the ionized molecule I_2^+ ($^2\Pi_{g,3/2}$, $^2\Pi_{g,1/2}$, $^2\Pi_{u,3/2}$, and $^2\Pi_{u,1/2}$, respectively) are studied, including correlation effects up to the CCSD(T) level of theory. In a second set of calculations the complete spectrum of all ionized states that dissociate into $I+I^+$ is calculated using the same approach as for the curves of the excited states. The assignment of the recently measured ''a'' state to a $^4\Sigma^-_{u,3/2}$ state by Cockett *et al.*[28] is discussed.

II. COMPUTATIONAL DETAILS

All calculations presented in this paper are performed using the fully relativistic *ab initio* MOLFDIR[47,48] program package, developed at the University of Groningen. Nonrelativistic Hartree–Fock (NR–HF) calculations are performed using the nonrelativistic option of the program package. The effect of the Gaunt[49] interaction, the magnetic part of the Breit[50] term that describes the magnetic interaction between electrons, is calculated in the MOLFDIR program package by perturbation theory applied to the Dirac–Hartree–Fock (DHF) wave function. The speed of light is taken to be 137.035 989 5 atomic units.

The molecular spinors of open-shell systems are generated using an average of configurations DHF.[46] Subsequently, a full CI is performed in the open-shell spinor space in order to project out the different states that arise from the open-shell manifold. This approach, which is denoted Complete Open Shell Configuration Interaction (COSCI), gives us a balanced description of all states in the manifold and their interaction. Correlation effects can be studied at different levels of theory. A Restricted Active Space Configuration Interaction (RASCI) program employing a similar partitioning of the active space as is done in the nonrelativistic case,[51] can be used for single- and multireference (MR) calculations. For the multireference CI we use the COSCI states as the reference wave functions. For closed shell systems and systems with a single reference determinant the RELCCSD program,[52] a relativistic Coupled Cluster Singles Doubles (CCSD) program,[53] is used. In this program the next higher-order terms, the triple excitations, can be included using three different noniterative corrections labeled $-T$,[54] (T),[55] and $+T$.[56] The RELCCSD program can also calculate the correlation energy based on second-order Møller–Plesset perturbation theory (MP2).

There are three classes of two-electron repulsion integrals in the DHF calculation, the (LL|LL) class of integrals, which are comparable to the nonrelativistic integrals, the (LL|SS) class that represents the two-electron spin–orbit interaction and the (SS|SS) class of integrals. This last class of integrals arises from the small component part of the wave function and contributes formally to order α^4 to the electronic energy. Since the small component density is mainly located in regions close to the respective nuclei this contribution has very small effect on the calculated valence properties. In fact, it can be shown[57,58] that the interatomic contribution of the (SS|SS) class of integrals can be represented by the Coulomb repulsion between the small component densities of the different atoms in the molecule. In calculating potential energy curves (Secs. IV A and V B), this large class of integrals can therefore be omitted and replaced by a small repulsive (electrostatic) contribution[58] $q_{S1}q_{S2}/R$ at each distance R, where q_{S1} and q_{S2} are the small component densities on atoms 1 and 2, respectively. The omission of these integrals in the iterative SCF process has only a small effect on the core spinors and no significant effect on the valence spinors.

For the nonrelativistic calculations a point-nucleus model is used, whereas for the relativistic calculations the nucleus is represented by a Gaussian charge distribution[59] with an exponential value of $1.845\,238\,916E+09$.

The iodine basis is the contracted pVTZ basis taken from Visscher.[60] The primitives are of triple zeta quality in the valence region and the contracted functions are generated using a modified[61,62] version of GRASP.[63]

The point groups D_{4h}, O_h, and their double groups (D^*_{4h} and O^*_h) are used in the calculations for the I_2 molecule and the I atom, respectively.

Equilibrium bond lengths (R_e) and vibration frequencies (ω_e) resulting from the single reference calculations on the ground state and the lowest ionized states are determined by a fourth-order polynomial fit to at least eight points of the potential energy curve. The polynomial obtained is used to calculate the anharmonicity constant with the MOLCAS[64] program VIBROT. The VIBROT program is also used to derive the spectroscopic properties of the potential energy curves of the excited and ionized states calculated with the COSCI approach. The dissociation energy of the ground state is calculated relative to the energy of the $^2P_{3/2}$ atomic state. The latter energy is obtained by optimizing the average energy of the $5p_{1/2})^2 5p_{3/2})^3$ configuration.

The notation σ_g, π_u, π_g, and σ_u is used for the molecular orbitals that can be formed as linear combinations of the six atomic $5p$ orbitals. The molecular spinor combinations are labelled by their dominant character $\sigma_{g,1/2}$, $\pi_{u,1/2}$, $\pi_{u,3/2}$, $\pi_{g,1/2}$, $\pi_{g,3/2}$, or $\sigma_{u,1/2}$. The other filled orbitals are not listed explicitly. In nonrelativistic calculations we can assign the molecular states using Λ–Σ coupling. In our relativistic calculations we work with intermediate coupling so only the ω and Ω quantum numbers apply. To connect to previous discussions on the assignment of states, and because the molecular spinors have relatively pure σ or π character, we have tried to analyze the calculated states in terms of Ω components of Λ–Σ states. This analysis is facilitated by comparing with a nonrelativistic calculation in a two-component spinor basis (using the nonrelativistic option of MOLFDIR). In this case we obtain pure $\sigma_{g,1/2}$, $\pi_{u,1/2}$, $\pi_{u,3/2}$, $\pi_{g,1/2}$, $\pi_{g,3/2}$, and $\sigma_{u,1/2}$ spinors. We can then analyze which Ω components of the Λ–Σ states contribute to a particular relativistic state by comparing the determinantal compositions of the (nonrelativistic) Λ–Σ states, which are also calculated in double group symmetry, with those of the relativistic Ω states. The molecular states are then labelled on the basis of the dominant Λ–Σ state. When the spinors do not have clear σ or π character, this analysis cannot be carried out, and only the Ω label is used. When there is no dominant

TABLE I. Overview of calculated spectroscopic properties for the iodine ground state. The calculated results are compared with experimental data and other theoretical work. All calculations have spin–orbit effects included.

Method[a]	CV[b]	R_e (Å)	D_e (eV)	ω_e (cm^{-1})	$\omega_e x_e$ (cm^{-1})
NR-HF	⋯	2.681	1.03	237	0.39
NR-HF+CCSD(T)	2	2.695	1.91	221	0.49
DHF	⋯	2.682	0.40	229	0.42
DHF+Gaunt	⋯	2.683	0.40	229	0.42
DHF+CCSD(T)	1	2.717	1.28	206	0.61
	2	2.699	1.39	210	0.59
	3	2.698	1.39	212	0.58
DHF+CCSD(T) (ext. basis)[c]	3	2.685	1.53	217	0.58
RECP, HF, MP2 (Ref. 34)		2.733	1.17	202	⋯
RECP, CASSCF, FOCI (Ref. 41)		2.770	1.45	210	⋯
PP, MCSCF (Ref. 35)		2.699	1.66	230	⋯
PP, MCSCF, MRCISD (Ref. 31)		2.769	0.76	185	0.80
PP+CPP, CISD (Ref. 32)		2.687	1.35	⋯	⋯
PP+CPP, CCSD(T) (Ref. 36)		2.668	1.57	215	⋯
DFT+GGC, ZORA (Ref. 37)		2.719	1.58	197	⋯
Experimental (Ref. 72)		2.666	1.55	214.5	0.61

[a]NR-HF (Nonrelativistic Hartree–Fock), DHF (Dirac–Hartree–Fock), RECP (relativistic effective core potential), PP (pseudopotential), CPP (core polarization potential), DFT+GGC, ZORA (Density functional plus gradient correction using the ZORA method).

[b]Active space used in the correlation calculations: 1: $5s$ core, $5p$ valence, and full virtual space; 2: $4d$ and $5s$ core, $5p$ valence, and full virtual space; 3: $4s$, $4p$, $4d$, and $5s$ core, $5p$ valence, and full virtual space.

[c]Basis extended with one g function; see the discussion at the end of Sec. III.

contribution from a particular Λ–Σ state we will label the state only by its Ω quantum number.

III. THE IODINE GROUND STATE

In this section results of calculations on the ground state properties of the iodine molecule are shown. The spinors are obtained by DHF calculations on the closed shell configuration $\sigma_g^2\pi_u^4\pi_g^4\sigma_u^0$. Relativistic as well as nonrelativistic calculations are performed to study the influence of relativity on the spectroscopic properties of the ground state. Electron correlation is included using the CCSD(T) method and core–valence effects are studied by including excitations from the $4s$, $4p$, $4d$, and $5s$ spinors.

A summary of the results is presented in Table I. The inclusion of relativistic effects results in a decrease in dissociation energy (D_e), which is mainly due to the spin–orbit splitting of the $^2P+^2P$ dissociation asymptote. The spin–orbit interaction is not completely quenched in the molecule, where a Mulliken population analysis gives a mixing of 2% of the antibonding $\sigma_{u,1/2}$ spinor into the occupied bonding $\pi_{u,1/2}$ spinor. The weakened molecular bond is, however, not accompanied by a substantial bond length expansion because scalar relativistic effects contract the spinors and almost cancel the spin–orbit effect on the R_e. The effect of the Gaunt term on the spectroscopic properties is negligible.

Core–valence correlation effects are studied by adding, in a number of stages, core spinors to the CCSD calculation. The inclusion of core spinors in the correlation calculation results in a shortening of the R_e by 0.02 Å and an increase of the D_e by 0.1 eV. Schwerdtfeger *et al.*[32] and Dolg[36] have performed calculations using relativistic pseudopotentials (PP) in which the core–valence effects are accounted for by a (semiempirical) core polarization term (CPP). They found effects of 0.03 Å and 0.06 eV and 0.03 Å and 0.09 eV, respectively, upon including core–valence correlation. The size of the core–valence effect calculated in this paper hence is in close agreement with the PP results.

There remains some discrepancy between the experimental and our calculated R_e and D_e. A better agreement with experimental data is obtained in the highly correlated calculations of Dolg.[36] Dolg performed HF and CCSD(T) calculations with a large uncontracted basis set, using a Douglas–Kroll–Hess[65,66] transformed Hamiltonian, where the spin–orbit (SO) term was included afterward. The HF+SO results from his calculations are in close agreement with the DHF results presented in this paper. His correlated results are better as a result of a larger basis set, which includes higher l functions. Dolg[67] also studied basis set effects by performing a series of PP calculations with an uncontracted basis set, where functions with increasing l values, up to g functions, were included. In these calculations it was found that the inclusion of g functions gives a contraction of the R_e by 0.02 Å at the CCSD(T) level. The basis set effects were also discussed by Teichteil and Pelissier,[31] and they observed that the inclusion of a g function has a larger effect than the inclusion of a second f function. We performed an additional set of calculations where one diffuse g function, with a judiciously chosen but not optimized exponential value of 0.22, was included. The CCSD(T) results show a reduction of R_e by 0.014 Å. Increases of 0.14 eV and 5 cm^{-1} are found for D_e and ω_e, respectively.

We conclude that the small discrepancies with experiment can be resolved by the extension of the basis set and

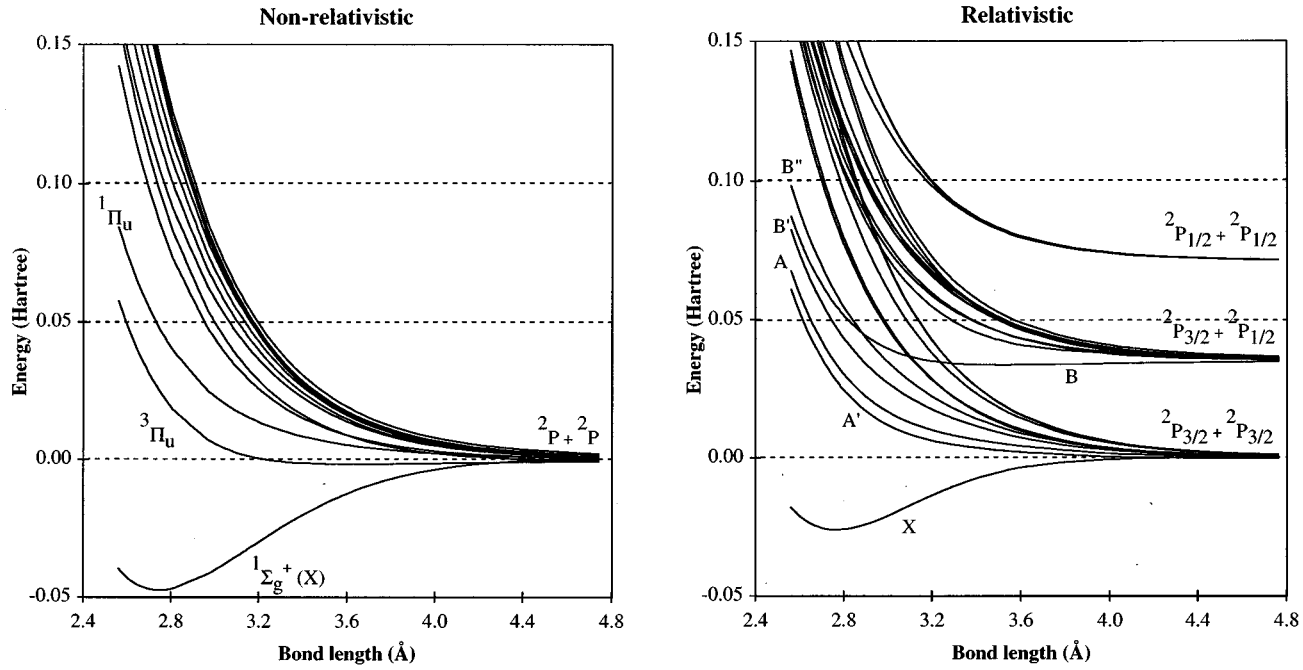

FIG. 1. Nonrelativistic (left) and relativistic (right) potential energy curves for the excited states of I_2 (states dissociating in two $5p^5\ ^2P$ iodine atoms are shown).

the inclusion of core–valence effects. For the work reported here such an extension of the basis set is impractical at present due to the large number of calculations necessary to obtain the potential energy curves of the excited and ionized states.

IV. THE EXCITED STATES OF IODINE

Potential energy curves of all states resulting from the $\sigma_g^k \pi_u^1 \pi_g^m \sigma_u^n$ configurations, where $k+1+m+n=10$, are calculated with the COSCI method using the average of configurations DHF spinors, with 10 electrons in 12 spinors.

The potential energy curves are calculated relativistically as well as nonrelativistically, using the nonrelativistic option in the MOLFDIR program package. For the nonrelativistic case, 24 states, of which 12 states dissociate into I^+ and I^-, are calculated. There are 43 states in the relativistic case with 20 states dissociating into ion-pair states. The results are presented and discussed in Sec. IV A. In Sec. IV B their accuracy is assessed by comparing them with the results of additional MRSDCI calculations, with the COSCI states as references.

A. Potential energy curves

The potential energy curves of the valence excited states that dissociate into the $^2P_J + {}^2P_J (J=3/2$ or $1/2)$ atomic states are derived from COSCI calculations at about 50 different bond distances. The resulting curves are presented in Fig. 1.

The D_e of the ground state (0.71 eV) obtained from the COSCI calculation is too small in comparison to the experimental value (1.55 eV) but larger than the single reference closed shell result (0.40 eV) of Sec. III because of the interaction with antibonding configurational states in the open-shell manifold that assure proper dissociation behavior. Potential curves of excited states that are known from experiment to be bonding are also found to be less bonding and sometimes even nonbonding. Using COSCI orbitals instead of state optimized orbitals to calculate the D_e for a closed shell wave function of the ground state yields results that are very similar to those reported in Sec. III. In line with what is generally observed when antibonding configurational states are included in the wave function (nondynamical correlation), the COSCI bond length of 2.76 Å for the ground state is larger than the single reference bond length of 2.68 Å. Core–valence correlation is probably the main ingredient necessary to shorten the R_e toward the experimental value of 2.66 Å. This is expected to improve the bond distances of the excited states, which are also found 0.1 Å too long, as well.

The splitting of the calculated states due to spin–orbit interaction agrees well with the observed splittings (see Table II). The important nondynamical correlation effects are apparently sufficiently described by a COSCI calculation in the spinor space spanned by the $5p$ spinors. The relative splitting of the states describing dissociated neutral atoms ($^2P_J + {}^2P_J$ with $J=1/2$ or $3/2$) is also in good agreement with experimental data.

The calculated potential energy curves and their spectroscopic properties can be compared with two other theoretical calculations in which the relativistic effects are introduced using relativistically optimized pseudopotentials. A two configurations MCSCF approach is employed by Teichteil and Pelissier[31] to calculate the ground state using the configurations $\sigma_g^k \pi_u^4 \pi_g^4 \sigma_u^n$ with $k+n=2$. Subsequently they generate one set of orbitals (using improved virtual orbitals) as a basis

TABLE II. Calculated nonrelativistic and relativistic vertical excitation energies (eV), at the experimental ground state equilibrium bond length, compared with experimental and other theoretical data. The notation $klmn$, used for the main configurations, is based on $\sigma_g^k \pi_u^1 \pi_g^m \sigma_u^n$.

Nonrelativistic		Relativistic					Ref. 31 Teichteil and Pelissier	Ref. 30 Mulliken
Λ–Σ states	COSCI	ω–ω states	COSCI	MR-CISD	Dominant configurations	Exp.		
$^1\Sigma_g^+$	0.00	(1) 0_g^+	0.00	0.00	2440	0.00	0.00	0.00
		(1) $2u$	1.78	1.75	2431	1.69[a,e]	1.65	1.66
$^3\Pi_u$	2.25	(1) $1u$	1.95	1.91	2431	1.84[a]	1.82	1.79
		(1) 0_u^-	2.34	2.30	2431	2.13[a,e]	2.18	2.34
		(1) 0_u^+	2.50	2.43	2431	2.37[b]	2.34	2.37
$^1\Pi_u$	2.92	(1) $1u$	2.72	2.62	2431	2.49[a,f]	2.57	2.38
		(1) $2g$	3.62	3.59	2341		3.45	3.2
$^3\Pi_g$	4.17	(1) $1g$	3.71	3.69	2341		3.56	3.4
		(2) 0_g^+	4.21	4.17	2341→2422[d]		4.09	4.1
		(1) 0_g^-	4.34	4.25	2341		4.08	4.1
$^1\Pi_g$	4.53	(3) $1g$	4.49	4.41	2341		4.27	4.1
$^3\Sigma_u^+$	4.17	(2) 0_u^-	4.64	4.64	1441		4.54	4.5
		(3) $1u$	4.71	4.67	1441	4.57[c]	4.58	4.57
$^3\Sigma_g^-$	5.03	(3) 0_g^+	4.36	4.29	2422→2341[d]		4.19	3.9
		(2) $1g$	4.84	4.71	2422		4.65	3.8
$^1\Delta_g$	5.30	(2) $2g$	5.07	4.98	2422		4.98	4.2
$^1\Sigma_g^+$	5.54	(4) 0_g^+	5.79	5.64	2422+2242[d]		5.65	4.4
$^1\Sigma_u^-$	5.87	(3) 0_u^-	5.02	5.10	2332		4.93	5.4
		(1) $3u$	5.00	5.11	2332		4.91	4.7
$^3\Delta_u$	5.95	(2) $2u$	5.66	5.73	2332		5.57	5.3
		(4) $1u$	6.34	6.38	2332		6.24	5.9
$^3\Sigma_u^+$	6.04	(5) $1u$	5.76	5.81	2332		5.64	5.5
		(4) 0_u^-	6.35	6.36	2332		6.25	5.6

[a]Reference 9.
[b]Reference 10.
[c]Reference 68.
[d]See the discussion in Sec. IV B.
[e]Values estimated by Tellinghuisen.
[f]The experimental value corresponds to a maximum absorption and is not strictly comparable to our vertical excitation energy.

for an additional MRCI calculation that includes spin–orbit matrix elements between the 23 states that dissociate into neutral atoms. Another route to calculate the potential energy curves and spectroscopic properties is taken by Li and Balasubramanian.[41] Here all states are generated in a CASSCF calculation with partially occupied $5s$ and $5p$ orbitals. Dynamical correlation is accounted for by means of additional MRCI calculations. The resulting potential energy curves are finally corrected for the effect of spin–orbit splitting by a limited MRCISD calculation using ground state orbitals.

The main features of the COSCI potential energy curves and their associated properties should be comparable to the results of these two methods discussed above. Especially, differences in the spin–orbit splitting of states should be minor. However, while our relativistic potential energy curves show a close resemblance to the curves generated by Teichteil and Pelissier, they differ from the curves calculated by Li and Balasubramanian.

A possible reason for this is the smaller CI space employed by Li and Balasubramanian. Teichteil and Pellisier perform a CI in a space that contains all states that dissociate into the neutral atoms (23 states). This CI space is identical with that of the COSCI calculations presented in this paper. In the spin–orbit MRCI calculations of Li and Balasubramanian, according to Table II of their paper, the configurations $\sigma_g^2 \pi_u^3 \pi_g^3 \sigma_u^2$, $\sigma_g^2 \pi_u^2 \pi_g^4 \sigma_u^2$ and the $1g$ and $2g$ components of $\sigma_g^2 \pi_u^4 \pi_g^2 \sigma_u^2$ are not included in the CI reference space. Since some of these configurations give rise to low lying states it may well be that omission of these configurations has a significant effect on the potential energy curves.

B. Vertical excitation energies

In Table II the calculated, relativistic, and nonrelativistic, vertical excitation energies are given at the experimental R_e of the ground state. The vertical excitation energies of states dissociating into neutral atoms, third column in Table II, are in reasonable agreement with experimental data. The vertical excitation energies of the ion-pair states (not included in Table II) are found to be 1.65 eV too high compared to experimental data. This shift is caused by the use of the configurational average DHF approach.

MRCISD calculations were performed to improve the vertical excitation energies and to examine the accuracy of the calculated spectrum. The $5s$-like spinors were placed in

the RAS1 space to allow for some core–valence correlation. The 12 active spinors were included in the RAS2 space and the virtuals with energies <2.5 hartree were placed in the RAS3 space. This gives a configuration space of eight million determinants that is reduced to one million determinants by using Abelian point group symmetry. The resulting vertical excitation energies are summarized in column 5 of Table II. No large differential effects are found in comparison to the DHF results.

In Table II the calculated vertical excitation energies are compared with those of Teichteil and Pelissier,[31] Mulliken's[30] predictions, and available experimental data. An assignment is given to the states based on their main character at the ground state R_e. The ordering of the states is consistent with the ordering found by Teichteil and Pelissier but differs from the one reported by Li and Balasubramanian.[41] For example, Li *et al.* find a reverse ordering for the $1g$ and $2g$ component of the low lying $^3\Pi_g$, and the 0_u^- component of the $^3\Sigma_u^+$ state (configuration 1441), which is found close to the $1u$ component of this state, is not present in their results.

There are also some differences in the ordering of the higher excited states when the results, presented here, are compared with those of Mulliken. We agree with Teichteil and Pelissier on the ordering of the states resulting from the 2422 and 1441 configurations and the differences found for the ungerade states could be a result of underestimated interactions between the $\omega-\omega$ states of the different configurations in the work of Mulliken.

Vertical excitation energies of the states $A'\ 2u$ ($^3\Pi_u$) and $B'\ 0_u^-$ ($^3\Pi_u$) were estimated from experimental data by Tellinghuisen.[9] The excitation energy of the A' state is in close agreement with the calculated value but the B' state is found too low in comparison with the results of Teichteil and Pelissier and those presented here. Comparing the differences between our vertical excitation energies and the experimentally estimated ones with those of Teichteil and Pellisier, we expect the experimental vertical excitation energy of the B' state to lie in between the value of Teichteil and Pellisier and our result.

The character of the $a'(2)0_g^+$ state has been discussed in various studies. We find an avoided crossing between $a'(2)0_g^+$ and (3) 0_g^+ at the ground state R_e, where the two states interchange $^3\Pi_g$ ($\sigma_g^2\pi_u^3\pi_g^4\sigma_u^1$) and $^3\Sigma_g^-(\sigma_g^2\pi_u^4\pi_g^2\sigma_u^2)$ character. This confirms the assignment of Teichteil and Pelissier. At shorter distances the $a'(2)0_g^+$ state has mainly $^3\Pi_g$ character and at longer distances it is dominated by the $^3\Sigma_g^-$ state. At the ground state R_e the contribution of both states is found to be 50%.

C. Empirically improved potential energy curves

The calculated vertical excitation energies of the states dissociating into neutral atoms agree rather well with the experimental data. The deviations are systematic, the calculated transition energies being all about 0.1 eV larger than the measured data. As noted in Sec. V A, the calculated bond lengths are also all systematically too large by about 0.1 Å.

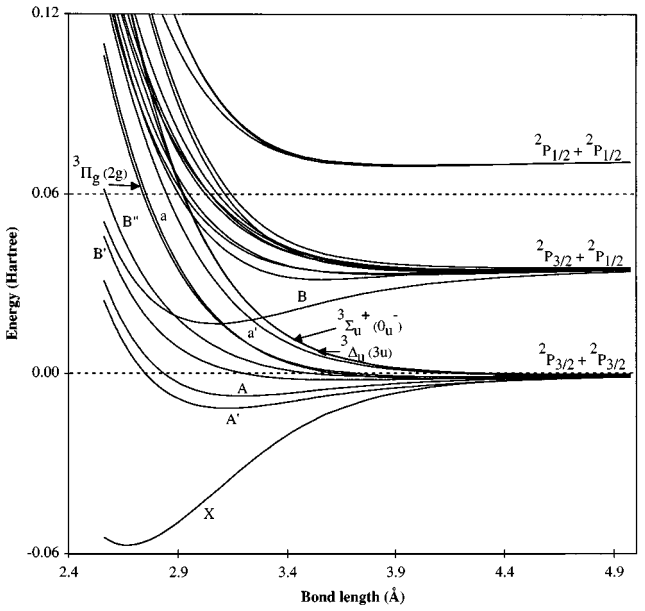

FIG. 2. Improved relativistic potential energy curves for the excited states of I_2. [States dissociating in two $5p^5\ ^2P_J(J=3/2,1/2)$ iodine atoms are shown.]

The D_e and ω_e, on the other hand, show less regular discrepancies when compared with the experimental data. The CCSD(T) results for the ground state show that extending the COSCI calculations such as to account for dynamical correlation could lead to substantial improvement. Such an extension, e.g., by a multireference CI method is, however, impractical to carry out for all excited states at all points of their potential energy curves. Following Teichteil,[69] improvement can be pragmatically obtained by a simple empirical correction to the ground state potential energy curve. An empirical RKR ground state is constructed[14] and the differences $\Delta E(R)$ between this curve and the calculated one are determined. The calculated energies at each point R of all excited states are then shifted by $\Delta E(R)$ and again fitted to a curve, as described before. The resulting corrected potential energy curves are shown in Fig. 2, together with their assignment. Table III displays the spectroscopic properties derived from these curves and it is seen that there is good agreement with the experimental data that is available for some of the states.

Much experimental work concerns the predissociation of the $B\ 0_u^+$ state. The potential energy curves of states, responsible for the predissociation processes, should be nearby or crossing the B state. The $B'(1)0_u^-$ state, which can be assigned as a $^3\Pi_u$, lies below the curve of the B state. States that cross the potential energy curve of the $B(^3\Pi_u)$ state, and that can contribute to predissociation of the B state, are the $B''1u$, $a1g$, $a'0_g^+$, and the $(2)0_u^-$, respectively. These four states all cross the B curve at a low vibrational level. We will now discuss the position, relative to the B state, and the character of these four states. The $B''1u$, which has $^1\Pi_u$ character crosses the inner limb of the B curve around the vibrational quantum numbers $\nu=4,5$, which is in agreement

TABLE III. Spectroscopic properties for the excited states of iodine (improved potential energy curves based on COSCI results). Experimental values and their references are given in parentheses.

State: ω–ω (Λ–Σ)	Dissociation products	D_e (eV)	T_e (eV)	r_e (Å)	ω_e (cm^{-1})	$\omega_e x_e$ (cm^{-1})
X:$0_g^+(^1\Sigma_g^+)$	$^2P_{3/2}+^2P_{3/2}$	1.556	0.000	2.666	214.5	0.65
	(Refs. 14, 68)					
A′:$2u(^3\Pi_u)$	$^2P_{3/2}+^2P_{3/2}$	0.316	1.241	3.123	100.9	0.85
	(Ref. 70)	(0.311)	(1.245)	(3.079)	(108.8)	(1.28)
A:$1u(^3\Pi_u)$	$^2P_{3/2}+^2P_{3/2}$	0.205	1.351	3.190	84.9	1.07
	(Ref. 71)	(0.203)	(1.353)	(3.129)	(88.3)	(1.55)
B′:$0_u^-(^3\Pi_u)$	$^2P_{3/2}+^2P_{3/2}$	0.057	1.499	3.648	30.9	1.20
	(Ref. 7)	(0.045)	(1.511)	(4.2)	(20.5)	(0.29)
a:$1g(^3\Pi_g)$	$^2P_{3/2}+^2P_{3/2}$	0.045	1.511	4.162	25.2	0.45
	(Ref. 13)	(0.037)	(1.505)	(4.311)	(23.6)	(0.48)
B″:$1u(^1\Pi_u)$	$^2P_{3/2}+^2P_{3/2}$	0.032	1.525	4.031	21.2	0.35
	(Ref. 12)	(0.022)	(1.534)	(4.2)	(19.8)	
$2g(^3\Pi_g)$	$^2P_{3/2}+^2P_{3/2}$	0.031	1.525	4.226	21.6	0.49
$3u(^3\Delta_u)$	$^2P_{3/2}+^2P_{3/2}$	0.013	1.543	4.756	13.9	0.79
a′:$(2)0_g^+$	$^2P_{3/2}+^2P_{3/2}$	0.012	1.544	4.681	15.1	0.85
	(Ref. 13)	(0.017)	(1.539)	(4.641)	(17.7)	(0.43)
$(2)0_u^-$	$^2P_{3/2}+^2P_{3/2}$	0.006	1.550	4.803	10.9	0.67
B:$0_u^+(^3\Pi_u)$	$^2P_{3/2}+^2P_{1/2}$	0.517	2.009	3.070	119.3	0.65
	(Ref. 14)	(0.543)	(1.955)	(3.024)	(125.7)	(0.76)
$(3)0_g^+$	$^2P_{3/2}+^2P_{1/2}$	0.114	2.412	3.563	72.9	1.02
	(Ref. 72)	(0.107)	(2.391)	(3.645)	(64.4)	(1.23)
$1g(^1\Pi_g)$	$^2P_{3/2}+^2P_{1/2}$	0.070	2.457	3.913	32.1	0.58
	(Ref. 29)	(0.058)	(2.441)	(4.05)	(29.6)	
$0_g^-(^3\Pi_g)$	$^2P_{3/2}+^2P_{1/2}$	0.058	2.468	3.851	32.7	0.60
b′:$2u(^3\Delta_u)$	$^2P_{3/2}+^2P_{1/2}$	0.040	2.486	4.183	25.7	0.61
	(Ref. 11)	(0.037)	(2.461)	(4.25)		
$1g(^3\Sigma_g^-)$	$^2P_{3/2}+^2P_{1/2}$	0.032	2.495	4.273	22.1	0.54
$(3)0_u^-$	$^2P_{3/2}+^2P_{1/2}$	0.029	2.497	4.319	20.7	0.48
C:$1u(^3\Sigma_u^+)$	$^2P_{3/2}+^2P_{1/2}$	0.029	2.497	4.322	20.8	0.51
$2g(^1\Delta_g)$	$^2P_{3/2}+^2P_{1/2}$	0.022	2.504	4.415	18.3	0.42
$1u(^3\Sigma_u^+)$	$^2P_{3/2}+^2P_{1/2}$	0.008	2.518	4.673	12.6	0.93
$0_g^+(^1\Sigma_g^+)$	$^2P_{1/2}+^2P_{1/2}$	0.054	3.442	3.928	33.8	0.91
$(4)0_u^-$	$^2P_{1/2}+^2P_{1/2}$	0.053	3.444	3.918	33.3	0.95
$1u(^3\Delta u)$	$^2P_{1/2}+^2P_{1/2}$	0.045	3.452	3.991	28.2	0.68

with the experimental findings.[15] The potential energy curve of the $a1g(^3\Pi_g)$ state crosses the B state at the outer limb close to the equilibrium distance ($\nu=0$). The $^3\Pi_g(2g)$ state lies close to the $a1g(^3\Pi_g)$ state and crosses this state below the crossing with the B state. The curves of the $a'0_g^+$ and the $(2)0_u^-$ state cross the outer limb of the B state curve at vibrational numbers around $\nu=2$ and $\nu=3,4$, respectively. The character of the $a'0_g^+$ state, which is mainly $^3\Sigma_g^-(\sigma_g^2\pi_u^4\pi_g^2\sigma_u^2)$ at the crossing point, has been discussed at the end of the previous section. Teichteil and Pelissier discussed the character of the $(2)0_u^-$ state and the interaction with the $(3)0_u^-$ and $(4)0_u^-$ states, resulting from the configurations $\sigma_g^2\pi_u^3\pi_g^3\sigma_u^2$ ($^1\Sigma_u^-$, $^3\Sigma_u^+$) and $\sigma_g^1\pi_u^4\pi_g^4\sigma_u^1$ ($^3\Sigma_u^+$). At short distances the $(2)0_u^-$ state has $^3\Sigma_u^+$ ($\sigma_g^1\pi_u^4\pi_g^4\sigma_u^1$) character, whereas the other two states have $\sigma_g^2\pi_u^3\pi_g^3\sigma_u^2$ ($^1\Sigma_u^-$, $^3\Sigma_u^+$) character. Around 2.78 Å an avoided crossing between the $(2)0_u^-$ state and the $(3)0_u^-$ state occurs, where the two states exchange their character. The $(2)0_u^-$ state shows mainly $\sigma_g^2\pi_u^3\pi_g^3\sigma_u^2$ ($^1\Sigma_u^-$, $^3\Sigma_u^+$) character at the crossing with the B state and at longer distances. These results are comparable with the ones found by Teichteil and Pelissier. An analysis of the singlet or triplet character of the two 0_u^- state resulting from the configuration $\sigma_g^2\pi_u^3\pi_g^3\sigma_u^2$, as was performed by Teichteil and Pelissier, is not straightforward to obtain due to the implicit interaction between the states in a relativistic description.

Tellinghuisen[10] performed experiments on a number of weakly bound states, $B'\,^3\Pi_u\,(0_u^-)$, $B''\,^1\Pi_u\,(1u)$, $a\,^3\Pi_g\,(1g)$, and $a'\,0_g^+$, and generated potential energy curves for the lower parts of these states. Only parts of the curves are known, other parts are estimated by extrapolation. Figure 3 shows a magnified picture of our calculated potential energy curves.

These curves are in good agreement with the findings of Tellinghuisen. The crossings of the $B''\,1u$ state with the $a\,1g$ state and the $a'\,0_g^+$ state are found to be around vibrational number $\nu=5$, 6 and $\nu=1$, 2, respectively.

Experimental data are available for a number of other states the assignment of which will now be discussed. The assignment of the $b'\,2u$ state to $a\,^3\Delta_u$ by Tellinghuisen[11] is confirmed by the calculations presented here. Ishiwata *et al.*[72] found a weakly bound state that can be assigned to the (3) 0_g^+ state. Its character has been discussed before in combination with the assignment of the a' state.

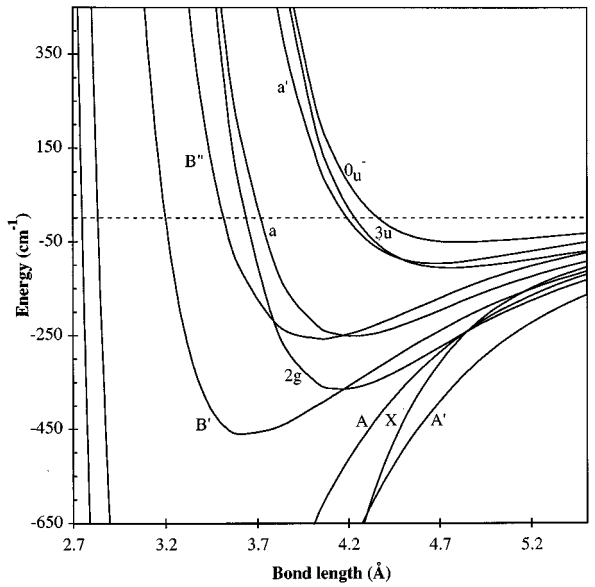

FIG. 3. Close up of the weakly bound states $B''\ ^1\Pi_u$, $a\ 1g$, $a'(0_g^+)$ and $(2)0_u^-$.

Viswanathan and Tellinghuisen[7] measured the spectroscopic properties of the $B'\ 0_u^-$ state ($^3\Pi_u$ character). They used a rough estimate for R_e to fit simulations of the experimental data, which differs somewhat from the one calculated in this work. Jewsbury *et al.*[29] determined spectroscopic properties for the $c\ 1g$ state and also discussed the character of this state. The character of the $c\ 1g$ state is mainly $^1\Pi_g$, which is in agreement with the experimental findings.

V. THE IONIZED STATES OF IODINE

Experimental spectroscopic data are available for the three lowest states of I_2^+, the ground states $(X)\ ^2\Pi_g\ (3/2g)$ and $^2\Pi_g\ (1/2g)$, and the first excited state $(A)\ ^2\Pi_u\ (3/2u)$. Assignment and interpretation of experimental data for the higher lying states is found to be more difficult due to the complexity of the spectrum. Of the higher lying states, only the vertical excitation energies of the A state $^2\Pi_u\ (1/2u)$ and B state $^2\Sigma_g^+\ (1/2g)$ have been identified. Very recently, Cockett *et al.*[28] determined the spectroscopic properties of a new state that they assigned to $a\ ^4\Sigma_u^-\ (3/2)$ on the basis of the only set of theoretically calculated potential energy curves available. To date there is only one set of theoretically calculated potential energy curves available.[41] Unfortunately this set shows rather large discrepancies with other experimental data.

We first present spectroscopic data for the lowest states calculated with a single reference approach. The first four states are described as single determinants with a hole in the $\pi_{g,1/2}$, $\pi_{g,3/2}$, $\pi_{u,1/2}$, or $\pi_{u,3/2}$ molecular spinor, respectively, the highest occupied spinors in their corresponding representations. The $^2\Sigma_g^+\ (1/2g)$ state is obtained by removing an electron from the highest occupied $\sigma_{g,1/2}$ spinor. The spinors resulting from DHF calculations on each of these states are used in subsequent CCSD(T) calculations in order to account for dynamical correlation corrections. The results of these calculations are discussed in Sec. V A.

Experimental data show that the higher lying states are thoroughly mixed by a spin–orbit interaction similar to what we have met in treating the neutral excited states. In Sec. V B we therefore use the COSCI approach, which allows us to study the mixing of the states in a balanced way. In the average of configuration open-shell DHF, all configurations resulting from all possible distributions of nine electrons over the $\sigma_g^k\pi_u^l\pi_g^m\sigma_u^n$ (where $k+l+m+n=9$) set of molecular spinors are taken into account. This means that the high lying states, which dissociate into a double cation (I^{2+}) and an ion (I^-), are included in the calculation. The data from the COSCI calculations are used to generate the potential energy curves of the ionized states. At the ground state equilibrium distance we have also carried out additional MRSDCI calculations, with the states from the COSCI calculation as references.

A. State optimized calculations

The potential energy curves for the four $^2\Pi$ states and the $^2\Sigma$ state are obtained by fitting the results of calculations on grids of at least nine points to a fourth-order polynomial. For the correlation calculations a total of 136 spinors is used, consisting of 103 virtual spinors (some high-energy solutions were not included) and 33 occupied spinors representing the $5s$ and $4d$ cores and the occupied $5p$ spinors. All calculations are performed relativistically as well as nonrelativistically. The results of calculations on the vertical ionization energy, ω_e and D_e are summarized in Table IV, where they are compared with the available experimental data and other theoretical work. Correlation has a large effect on properties like the ω_e and the R_e, but the effect on the spin–orbit splitting is small.

We will now discuss our results for the three spectroscopic properties presented and compare them with the available experimental data and other theoretical results. The vertical ionization energies are calculated at the experimental ground state R_e. The spin–orbit splittings of the $^2\Pi_g\ (3/2)$ and $^2\Pi_g\ (1/2)$ states agree well with the experimental data. The splitting of the $^2\Pi_u$ states is larger than the splitting of the $^2\Pi_g$ states but smaller than the measured values. This larger spin–orbit splitting of the $^2\Pi_u$ states was partially explained by Dyke *et al.*[42] They attribute the difference to the off-diagonal spin–orbit interaction between the $\pi_{1/2}$ and $\sigma_{1/2}$ spinors for gerade and ungerade states, an interaction that is inherently accounted for in a fully relativistic approach. The differences between the calculated and measured spin–orbit splittings must therefore be attributed to multireference effects (see the end of this section). Li and Balasubramanian,[41] using a multireference approach, however, find the spin–orbit splitting of the $^2\Pi_u$ states smaller than the splitting of the $^2\Pi_g$ states (0.63 and 0.76 eV, respectively).

The ω_e calculated for the $^2\Pi_g$ states and the $^2\Pi_u\ (3/2)$ state compare well with the accurate ZEKE-PFI experiments of Cockett *et al.*[24,28] No ω_e for the $^2\Pi_u\ (1/2)$ state is deduced from these experiments. From threshold photoelectron

TABLE IV. Calculated vertical ionization energy (I_ν), ω_e and R_e for the four lowest states of I_2^+, compared with experimental and other theoretical data.

Property	Method	$^2\Pi_g(3/2)$	$^2\Pi_g(1/2)$	$^2\Pi_u(3/2)$	$^2\Pi_u(1/2)$	$^2\Sigma_g^+$
I_ν (eV)[a]	NR-HF	9.36		11.54		12.12
	DHF	8.94	9.51 (0.57)	11.10 (2.16)	11.85 (2.91)	12.18 (3.24)
	DHF+CCSD(T)	9.13	9.74 (0.62)	10.97 (1.84)	11.65 (2.52)	12.77 (3.64)
	Li *et al.* (Ref. 41)	8.62	9.38 (0.76)	10.19 (1.57)	10.82 (2.20)	⋯
	Experiment (Ref. 24)	9.31	9.95 (0.64)	⋯	⋯	⋯
	Experiment (Ref. 23)	9.34	9.98 (0.64)	10.96 (1.62)	11.81 (2.47)	12.95 (3.61)
ω_e (cm^{-1})	NR-HF	277		211		124
	DHF	270	233	199	207	174
	DHF+CCSD(T)[b]	238	227	140	156	⋯
	Li *et al.* (Ref. 41)	217	208	132	112	72
	Experiment (Refs. 24, 28)	240 (±1)	230 (±2)	138 (±2)	⋯	⋯
	Experiment (Ref. 23)	220 (±8)	214 (±8)	Average 128 (±8)		⋯
R_e (Å)	NR-HF	2.575		2.805		3.043
	DHF	2.571	2.604	2.820	2.804	2.921
	DHF+CCSD(T)[b]	2.613	2.626	2.949	2.910	⋯
	Li *et al.* (Ref. 41)	2.69	2.69	3.09	3.11	3.62
	Experiment (Ref. 22)	2.58	2.58	2.99	2.98	⋯

[a]Relative energies are given in parentheses.
[b]Correlated potential energy curve of the $^2\Sigma_g^+$ state has large mixing with other states and cannot be studied with the CCSD(T) method.

spectroscopy[23] only an averaged frequency for the two $^2\Pi_u$ states is available. The frequencies reported for the gerade states are lower than found in the newer ZEKE-PFI results. Li *et al.* arrive at a frequency for the $^2\Pi_u$ (1/2) state that is 20 cm^{-1} smaller than that of the $^2\Pi_u$ (3/2) state, which is similar to the results of Boerrigter *et al.*[73] for the Br_2^+ molecule. This shift is attributed to the spin–orbit allowed mixing with nearby states, for example, the large mixing of the $^2\Pi_u$ (1/2) with *a* $^2\Sigma_u^+$ (1/2) state. Such mixing cannot be accounted for in single reference CCSD(T).

The calculated R_e are presented in the last part of Table IV. Based on the bonding character of the orbitals of the neutral molecule, the bond lengths of the four Π states are expected to be ordered as $^2\Pi_g$ $(3/2g) < {}^2\Pi_g$ $(1/2g) \ll {}^2\Pi_u$ $(1/2u) < {}^2\Pi_u$ $(3/2u)$. Through spin–orbit interaction the bonding $\pi_{u,1/2}$ spinor acquires antibonding character by mixing in of the $\sigma_{u,1/2}$, whereas the $\pi_{u,3/2}$ remains a pure bonding spinor. Therefore the $^2\Pi_u$ (1/2) will have a shorter R_e than the $^2\Pi_u$ (3/2) state. The antibonding $\pi_{g,1/2}$ spinor gets some bonding character from the $\sigma_{g,1/2}$ spinor, yielding a longer R_e for the $^2\Pi_g$ (1/2) state compared to $^2\Pi_g$ (3/2). This ordering is indeed found (see Table IV) and is in agreement with bond lengths estimated from experimental data.

We mentioned earlier that the properties of the $^2\Pi_u$ (1/2) state will be affected by nondynamical correlation in a way similar to that discussed for Br_2^+ by Boerrigter *et al.*[73] The $^2\Sigma_g^+$ state, which lies even higher in the spectrum, is expected to be heavily influenced by these effects and it has therefore not been discussed as yet. From CCSD correlation calculations, information on the growing importance of a nondynamical correlation can be estimated using the T1 diagnostic value.[74] For the two $^2\Pi_g$ states and the $^2\Pi_u$ (3/2) state the diagnostic values are small, whereas the values of the $^2\Pi_u$ (1/2) state reaches the critical values proposed in various papers. The T1 diagnostic values of the (*B*) $^2\Sigma_g^+$ state become very large (0.05–0.06) when going to distances longer than the ground state equilibrium distance and the calculated correlated results are hence unreliable. For this reason the correlated results of the relativistically calculated ω_e and R_e are not presented here. When nondynamical correlation becomes important, one requires a multireference description from the start. In Sec. V B, the effects of a multireference description will be studied using an average of configuration approach in which all the states are explicitly included in the calculations.

B. The potential energy curves of ionized iodine

The nonrelativistic and relativistic potential energy curves of the states that dissociate into the atom and its cation ($I+I^+$) are obtained from COSCI calculations for about 50 different bond distances. In Figs. 4 and 5 the nonrelativistic and relativistic potential energy curves for the lowest ionized states are presented, grouped by their parity. Extensive configuration interaction, due to spin–orbit coupling, is found, which makes it difficult to assign Λ–Σ state characters to the potential energy curves. The low lying states can still be identified but the complexity increases when one goes to states higher up in the spectrum. Hunds case (c) notation will be used except for those states that have clear Λ–Σ character.

The relative energies of the calculated dissociation limits for the states dissociating into the neutral atom and its cation are in close agreement with numerical atomic calculations (errors less than 0.05 eV). To discuss the assignment of experimentally determined states, the spectroscopic properties of the potential energy curves are calculated. These properties show discrepancies from experimental data similar to those discussed for the excited states of the neutral molecule, and here too improvement is obtained by applying a simple empirical correction to the lowest potential energy curve (see Section IV C). No RKR curve is known for the $^2\Pi_g(3/2)$

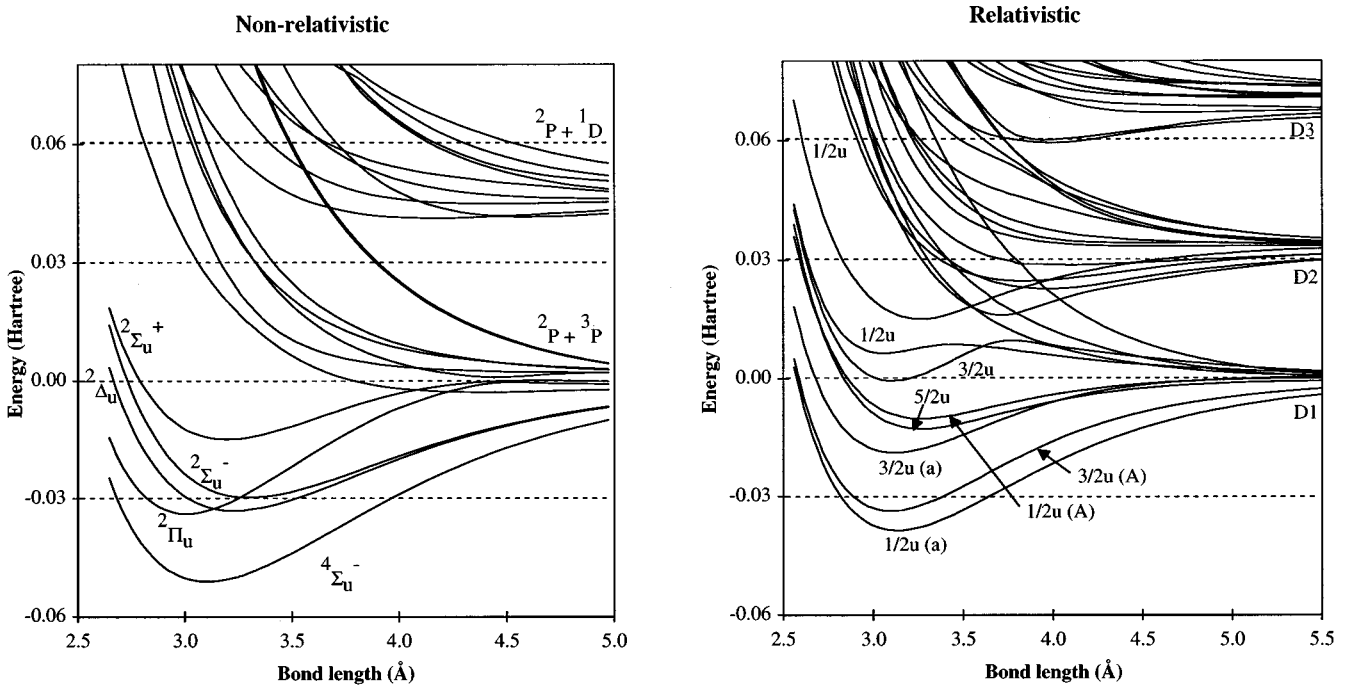

FIG. 4. Nonrelativistic (left) and relativistic (right) potential energy curves for the lowest ungerade states of I_2^+. Relativistic dissociation limits: $D1 = {}^2P_{3/2} + {}^3P_2$; $D2 = {}^2P_{3/2} + {}^3P_0$, ${}^2P_{3/2} + {}^3P_1$, and ${}^2P_{1/2} + {}^3P_2$; $D3 = {}^2P_{1/2} + {}^3P_0$, ${}^2P_{1/2} + {}^3P_1$, and ${}^2P_{3/2} + {}^1D_2$.

ionized state, and therefore a Morse potential, based on the experimental data of Cockett *et al.*,[24,28] is used for the correction. The properties of some of these improved curves, calculated using the VIBROT program of the MOLCAS[64] package, and the vertical excitation energies are collected in Table V. These properties are expected to be less accurate than those calculated for the excited states of the neutral molecule because of the simple Morse form used for the correction.

The vertical ionization energies are calculated at the ex-

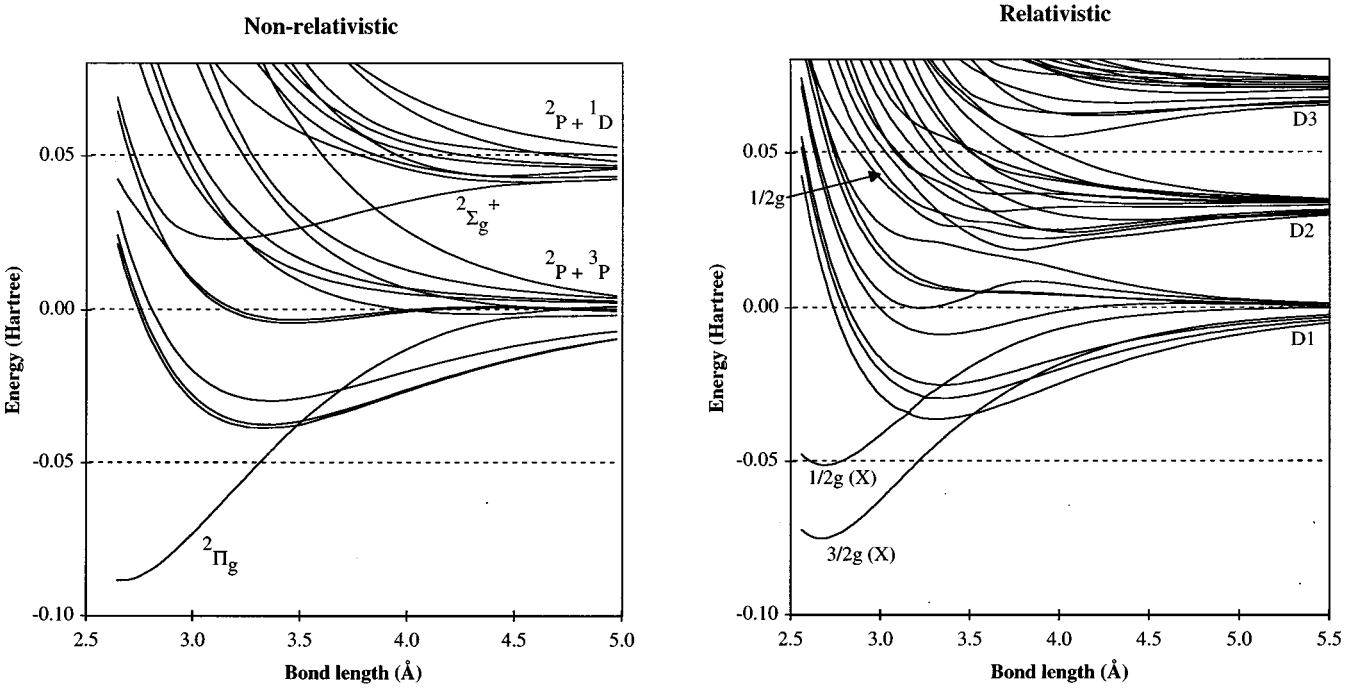

FIG. 5. Nonrelativistic (left) and relativistic (right) potential energy curves for the lowest gerade states of I_2^+. Relativistic dissociation limits: $D1 = {}^2P_{3/2} + {}^3P_2$; $D2 = {}^2P_{3/2} + {}^3P_0$, ${}^2P_{3/2} + {}^3P_1$, and ${}^2P_{1/2} + {}^3P_2$; $D3 = {}^2P_{1/2} + {}^3P_0$, ${}^2P_{1/2} + {}^3P_1$, and ${}^2P_{3/2} + {}^1D_2$.

TABLE V. Relative vertical ionization energies of some selected low lying states of the I_2^+ molecule. For a number of states other properties are also given. The notation $klmn$, used for the main configurations, is based on $\sigma_g^k \pi_u^1 \pi_g^m \sigma_u^n$.

State symm. ω–ω	Relative vertical ionization energy (eV) COSCI	MRCISD	Exp. (Ref. 23)	Li *et al.* (Ref. 41)	D_e (eV)	ω_e (cm^{-1})	$\omega_e x_e$ (cm^{-1})	Assignment and main configurations (Λ–Σ)
3/2*g*	0.00	0.00	0.00	0.00	2.70	240	0.69	*X*: 2430 ($^2\Pi_g$)
1/2*g*	0.65	0.63	0.64	0.76	2.03	230	0.76	*X*: 2430 ($^2\Pi_g$)
1/2*u*	1.64	1.68			1.38	137	0.29	*a*: 2421 ($^4\Sigma_u^-$)
3/2*u*	1.71	1.68	1.62	1.57	1.26	141	0.32	*A*: 2340 ($^2\Pi_u$)+ 2421 ($^4\Sigma_u^-$)
3/2*u*	2.09	2.06			0.85	133	0.37	*a*: 2421 ($^4\Sigma_u^-$)+ 2340 ($^2\Pi_u$)
1/2*g*	2.44	2.50			1.23	242		2331
1/2*u*	2.55	2.44	2.47	2.22	0.56	117	0.38	*A*: 2340 ($^2\Pi_u$)+ 2421
3/2*u*	2.57	2.56			0.62	120	0.38	2421 ($^2\Delta_u$)
1/2*g*	2.68	2.81						2331
1/2*g*	3.69	3.67						2331
1/2*g*	3.85	3.88						2331+ 1440 ($^2\Sigma_g^+$)
1/2*g*	3.97	3.76	3.61	3.46				*B*: 1440 ($^2\Sigma_g^+$)+ 2331

perimental R_e of the ground state. MRCISD calculations are performed to study the effects of dynamical correlation and relaxation on the vertical ionization energies and thereby on the position of the potential energy curves. The CI contains the antibonding $5s$ spinor in RAS1, the $5p$ spinors in RAS2 (i.e., the states from the COSCI calculation), and 96 virtual spinors in RAS3. The latter number encompasses all virtuals except for those with energies higher than 4 hartree. Determinants resulting from all single and double excitations between the different spaces are included. This results in a CI space of nine million determinants that is reduced to one million by using Abelian point group symmetry. The calculated vertical ionization energies of the four low lying Π states as well as the spin–orbit splitting are in close agreement with the experimental findings. Only small correlation effects are found for the two (X) $^2\Pi_g$ states and their spectroscopic properties are in close agreement with the single reference results in Sec. V A. For the (A) $^2\Pi_u$ states a considerable admixture of states from different configurations is found. This mixing does not affect the properties of the $^2\Pi_u(3/2)$ state, which are still close to the results of the single reference calculation in Sec. V A, but it has a large influence on the ω_e of the $^2\Pi_u(1/2)$ state. This quantity is now 24 cm^{-1} smaller than the value found for the $^2\Pi_u(3/2)$ state, which is in better agreement with the multireference approach of Li *et al.*[41]

With the calculated data one can now discuss the assignments of these states as they were made by Cockett *et al.*[28] and in the theoretical work of Li and Balasubramanian. We will first discuss the assignment of the ungerade states (A) $^2\Pi_u(3/2)$, (A) $^2\Pi_u(1/2)$, and a $^2\Pi_u(1/2)$ and after that we will consider the gerade states including the ground state. Boerrigter *et al.*[73] attributed the large difference in the ω_e of the two $^2\Pi_u$ states for the Br_2^+ molecule to the difference, induced by spin–orbit coupling, in the configuration interaction with states from the $\sigma_g^2 \pi_u^4 \pi_g^2 \sigma_u^1$ configuration, i.e. between the $^2\Sigma_u^+(1/2)$ and the $^2\Pi_u(1/2)$ states on the one hand and the $^2\Delta_u(3/2)$ and $^2\Pi_u(3/2)$ states on the other. A similarly large difference between the ω_e of the two $^2\Pi_u$ states is found in our calculations on I_2^+ and was also reported by Li *et al.*[41] However, we find that the properties of the $^2\Pi_u(1/2)$ state are influenced by the $^2\Sigma_u^+(1/2)$ state, whereas these authors find an interaction with the $^4\Sigma_u^-(1/2)$ state. They also find that the $^2\Pi_u(3/2)$ state is unperturbed while our calculations show a strong interaction with the $^4\Sigma_u^-(3/2)$ state. This interaction was suggested earlier, based on experimental data, by Jungen,[44] Leach,[21] and Mason and Tuckett.[22] At larger bond lengths (above 2.9 Å) the $^2\Pi_u(3/2)$ state starts to interact with the $^2\Delta_u(3/2)$ state, as found in the Br_2^+ molecule by Boerrigter *et al.*

Cockett *et al.* measured two ungerade states, ''*a*'' and ''*A*,'' with ionization energies that differ only by 0.05 eV, which they assigned to $^4\Sigma_u^-(3/2)$ and $^2\Pi_u(3/2)$, respectively. We find the lowest ungerade state to be $^4\Sigma_u^-(1/2)$ with a state of $3/2u$ symmetry just 0.07 eV above it. A second state of this symmetry is found at 0.38 eV above the $^4\Sigma_u^-(1/2)$ state. Both states are mixtures of $^2\Pi_u(3/2)$ and $^4\Sigma_u^-(3/2)$ at the ground state R_e, with the lowest $3/2u$ state having a somewhat larger $^2\Pi_u(3/2)$ character. The character of the two $3/2u$ states reverses when going to longer distances, giving a lower state with more $^4\Sigma_u^-(3/2)$ character, and the higher $3/2u$ state now also has considerable contributions from the $^2\Delta_u(3/2)$ state.

The calculated D_e and ω_e are in reasonable agreement with the experimental data of Cockett *et al.*, considering the

approximations that were made. On the basis of the relative positions of the potential energy curves and the agreement with the calculated spectroscopic properties (Table V), we assign the ''*a*'' state, measured by Cockett *et al.*, to $^4\Sigma_u^-(1/2)$. The measured *A* state is assigned to a mixed state of $^2\Pi_u(3/2)$ and $^4\Sigma_u^-(3/2)$ character.

We will now turn to the three measured states with gerade symmetry, the two $(X)\ ^2\Pi_g$ states and the $(B)\ ^2\Sigma_g^+$ state. From the calculated properties of the improved potential energy curves that agree closely with experimental results one can easily assign the $^2\Pi_g$ states.

The $(B)\ ^2\Sigma_g^+$ state, resulting from the $\sigma_g^1\pi_u^4\pi_g^4$ configuration, nonrelativistically (Fig. 5) dissociates into the atomic states $^1D+^2P$. In the nonrelativistic calculations an avoided crossing with a $^2\Sigma_g^+$ state from the $\sigma_g^2\pi_u^4\pi_g^2\sigma_u^1$ configuration is found at a short distance, where these states exchange their character. The potential energy curve of the *B* state crosses a large number of states that could interact with this state through spin–orbit coupling. Extensive mixing is indeed found in the relativistic calculations. The vertical excitation energy of the $B\ ^2\Sigma_g^+$ state is 0.35 eV higher than the experimental value. Some improvement is found when a MRCISD calculation is performed on top of the COSCI calculations, but the value is still 0.15 eV above the experimental value. Extensive correlation calculations on the whole potential energy curve of the *B* state, and most of the higher lying ionized states, are required to be able to discuss the detailed form of the potential energy curve presented by Leach. Li *et al.* found a global maximum at longer distances, one of the features of the potential energy curve suggested by Leach. This global maximum is also found in our empirically improved potential energy curve(s), but we cannot exclude that the missing large correlation corrections may considerably influence the form and position of the potential energy curve.

VI. CONCLUSIONS

The spectroscopic properties and potential energy curves of the ground state and the most important excited and ionized states of I_2 are calculated within a four-component relativistic framework. For the ground state relativity and correlation must be included in order to get results that are in close agreement with experimental data. It is shown that the remaining differences between the experimental and calculated relativistic values can be attributed to basis set effects and core–valence correlation effects. Core–valence correlation, by including excitations from the $4s$, $4p$, $4d$, and $5s$ spinors, results in a bond length contraction of 0.02 Å, comparable to the 0.03 Å that was obtained from semiempirical corrected pseudopotentials.

The spectroscopic properties of the set of excited states that dissociate into neutral atoms are well described when the calculated potential energy curves are collectively subjected to a simple empirical correction proposed by Teichteil.[68] Our calculated vertical excitation energies agree closely with those of Teichteil and Pelissier[31] but differ from the results of Li and Balasubramanian.[41] We have analyzed the position and character of the states $B''\ 1u$, $a\ 1g$, $a'0_g^+$, and 0_u^- that are responsible for the predissociation of the *B* state. The character of the a' state at the crossing point is $^3\Pi_g$ but at shorter bond distances this state has $^3\Sigma_g^-$ character due to an avoided crossing. For the (2) 0_u^- state we also find an avoided crossing resulting in $\sigma_g^1\pi_u^4\pi_g^4\sigma_u^1(^3\Sigma_u^+)$ character at short bond distances and $\sigma_g^2\pi_u^3\pi_g^3\sigma_u^2(^1\Sigma_u^-,^3\Sigma_u^+)$ character at longer distances which include the crossing point with the *B* state. These results corroborate the findings of Teichteil and Pelissier. The potential energy curves of some weakly bound states are in close agreement with the deductions from experiment of Tellinghuisen.[10]

For the ionized states, the spectroscopic properties of the two $(X)\ ^2\Pi_g$ states are well reproduced by our calculations. Nondynamical correlation effects must be included in order to obtain good results for the properties and the spin–orbit splitting of the two $(A)\ ^2\Pi_u$ states. We find that the $^2\Pi_u(3/2)$ state strongly interacts with the $^4\Sigma_u^-(3/2)$ state arising from the configuration $\sigma_g^2\pi_u^4\pi_g^2\sigma_u^1$, whereas the $^2\Pi_u(1/2)$ state mixes with the $^2\Sigma_u^+(1/2)$ state of this configuration. This differs from the analysis of Li *et al.* A new state measured by Cockett *et al.*[28] is reassigned to the (unperturbed) $^4\Sigma_u^-(1/2)$ based on the calculated spectroscopic properties. The first ''*A*'' state is assigned to a mixed state of $^2\Pi_u(3/2)$ and $^4\Sigma_u^-(3/2)$. Extensive correlation treatment and multiconfiguration calculations are required to obtain good potential energy curves for higher ionized states, like the $(B)\ ^2\Sigma_g^+$, of iodine.

ACKNOWLEDGMENTS

The authors thank Dr. Michael Dolg (MPI PKS Dresden) for providing results prior to publication and for enlightening discussions. Dr. Martin Cockett (University of York) and Dr. Kenneth Lawley (University of Edinburgh) are acknowledged for their comments on the I_2^+ results. This work was sponsored by the Netherlands Foundation for Chemical Research (SON) and the Stichting Nationale Computerfaciliteiten (National Computing Facilities Foundation, NCF) for the use of supercomputer facilities, both with financial support from the Nederlandse Organisatie voor Wetenschappelijk Onderzoek (Netherlands Organization for Scientific Research, NWO). LV wishes to acknowledge a Cray Research Grant and support from the Training and Mobility of Researchers programme (Contract No. ERBFMBICT960738) of the European Union.

[1] P. B. Beeken, E. A. Hanson, and G. W. Flynn, J. Chem. Phys. **78**, 5892 (1983).
[2] F. W. Dalby, C. D. P. Levy, and J. Vanderlinde, Chem. Phys. **85**, 23 (1984).
[3] B. J. Sullivan and D. A. Dows, Chem. Phys. **46**, 231 (1980).
[4] J. Vigué, M. Broyer, and J. C. Lehmann, J. Phys. **42**, 949 (1981).
[5] J. Vigué, M. Broyer, and J. C. Lehmann, J. Phys. **42**, 961 (1981).
[6] R. J. LeRoy, J. Chem. Phys. **52**, 2678 (1970).
[7] K. S. Viswanathan and J. Tellinghuisen, J. Mol. Spectrosc. **101**, 285 (1983).
[8] J. Tellinghuisen, J. Chem. Phys. **57**, 2397 (1972).
[9] J. Tellinghuisen, J. Chem. Phys. **58**, 2821 (1973).
[10] J. Tellinghuisen, J. Chem. Phys. **76**, 4736 (1982).
[11] J. Tellinghuisen, J. Chem. Phys. **87**, 5136 (1983).
[12] J. Tellinghuisen, J. Chem. Phys. **82**, 4012 (1985).

[13] S. Churassy, F. Martin, R. Bacis, J. Vergès, and R. W. Field, J. Chem. Phys. **75**, 4863 (1981).
[14] F. Martin, R. Bacis, S. Churassy, and J. Vergès, J. Mol. Spectrosc. **116**, 71 (1986).
[15] G. D. Chapman and P. R. Bunker, J. Chem. Phys. **57**, 2951 (1972).
[16] K. P. Lawley, T. Ridley, Z. Min, P. J. Wilson, M. S. N. Al-Kahali, and R. J. Donovan, Chem. Phys. **197**, 37 (1995).
[17] D. C. Frost, C. A. McDowell, and D. A. Vroom, J. Chem. Phys. **46**, 4255 (1967).
[18] S. Evans and A. F. Orchard, Inorg. Chim. Acta **5**, 81 (1970).
[19] A. B. Cornford, D. C. Frost, C. A. McDowell, J. L. Ragle, and I. A. Stenhouse, J. Chem. Phys. **54**, 2651 (1971).
[20] J. H. D. Eland, J. Chem. Phys. **70**, 2926 (1979).
[21] S. Leach, J. Phys. Chem. **92**, 5373 (1988).
[22] S. M. Mason and R. P. Tuckett, Chem. Phys. Lett. **160**, 575 (1989).
[23] A. J. Yencha, M. C. R. Cockett, J. G. Goode, R. J. Donovan, A. Hopkirk, and G. C. King, Chem. Phys. Lett. **229**, 347 (1994).
[24] M. C. R. Cockett, J. G. Goode, K. P. Lawley, and R. J. Donovan, J. Chem. Phys. **102**, 5226 (1995).
[25] J. P. Horner and J. H. D. Eland, Chem. Phys. Lett. **110**, 29 (1984).
[26] H. Van Lonkhuyzen and C. A. De Lange, Chem. Phys. **89**, 313 (1984).
[27] B. R. Higginson, D. R. Loyd, and P. J. Roberts, Chem. Phys. Lett. **19**, 480 (1973).
[28] M. C. R. Cockett, R. J. Donovan, and K. P. Lawley, J. Chem. Phys. **105**, 3347 (1996).
[29] P. J. Jewsbury, T. Ridley, K. P. Lawley, and R. J. Donovan, J. Mol. Spectrosc. **157**, 33 (1993).
[30] R. S. Mulliken, J. Chem. Phys. **55**, 288 (1971).
[31] C. Teichteil and M. Pelissier, Chem. Phys. **180**, 1 (1994).
[32] P. Schwerdtfeger, L. v. Szentpály, K. Vogel, H. Silberbach, H. Stoll, and H. Preuss, J. Chem. Phys. **84**, 1606 (1986).
[33] C. Y. Yang, Chem. Phys. Lett. **41**, 588 (1976).
[34] S. Y. Lee and Y. S. Lee, Chem. Phys. Lett. **187**, 302 (1991).
[35] G. Das and A. C. Wahl, J. Chem. Phys. **69**, 53 (1978).
[36] M. Dolg, Mol. Phys. **88**, 1645 (1996).
[37] E. Van Lenthe, Ph.D. thesis, Free University of Amsterdam, 1996.
[38] J. Vigué, M. Broyer, and J. C. Lehmann, J. Phys. **42**, 937 (1981).
[39] M. N. Glukhovtsev, A. Pross, M. P. McGrath, and L. Radom, J. Chem. Phys. **103**, 1878 (1995).
[40] M. Saute and M. Aubert-Frécon, J. Chem. Phys. **77**, 5639 (1982).
[41] Q. Li and K. Balasubramanian, J. Mol. Spectrosc. **138**, 162 (1989).
[42] J. M. Dyke, G. D. Josland, J. G. Snijders, and P. M. Boerrigter, Chem. Phys. **91**, 419 (1984).
[43] K. Wittel, Chem. Phys. Lett. **15**, 555 (1972).
[44] M. Jungen, Theor. Chim. Acta **27**, 33 (1972).
[45] E. Van Lenthe, E. J. Baerends, and J. G. Snijders, J. Chem. Phys. **99**, 4597 (1993).
[46] O. Visser, L. Visscher, P. J. C. Aerts, and W. C. Nieuwpoort, J. Chem. Phys. **96**, 2910 (1992).
[47] MOLFDIR, P. J. C. Aerts, O. Visser, L. Visscher, H. Merenga, W. A. de Jong, and W. C. Nieuwpoort, University of Groningen, The Netherlands, 1995.
[48] L. Visscher, O. Visser, P. J. C. Aerts, H. Merenga, and W. C. Nieuwpoort, Comput. Phys. Commun. **81**, 120 (1994).
[49] J. A. Gaunt, Proc. R. Soc. London Ser. A **122**, 513 (1929).
[50] G. Breit, Phys. Rev. **34**, 553 (1929).
[51] J. Olsen, B. O. Roos, P. Jørgensen, and H. J. A. Jensen, J. Chem. Phys. **89**, 2185 (1988).
[52] RELCCSD, L. Visscher, T. J. Lee, and K. G. Dyall, NASA Ames Research Center, Moffett Field, CA, 1995.
[53] L. Visscher, K. G. Dyall, and T. J. Lee, Int. J. Quantum Chem. Quantum Chem. Symp. **29**, 411 (1995).
[54] M. Urban, J. Noga, S. J. Cole, and R. J. Bartlett, J. Chem. Phys. **83**, 4041 (1985).
[55] K. Raghavachari, G. W. Trucks, J. A. Pople, and M. Head-Gordon, Chem. Phys. Lett. **157**, 479 (1989).
[56] M. J. O. Deegan and P. J. Knowles, Chem. Phys. Lett. **227**, 321 (1994).
[57] This idea was first presented by L. Visscher at the REHE workshop in Tromsø (1995) and is supported by subsequent calculations by T. Saue, Ph.D. thesis, University of Oslo, 1991.
[58] L. Visscher, Theor. Chem. Acc. (in press).
[59] L. Visscher and K. G. Dyall, At. Data Nucl. Data Tables (in press).
[60] L. Visscher and K. G. Dyall, J. Chem. Phys. **104**, 9040 (1995).
[61] K. G. Dyall and K. J. Faegri, Theor. Chim. Acta **94**, 39 (1996).
[62] Additional modifications by T. Saue and L. Visscher interfacing program with MOLFDIR.
[63] K. G. Dyall, I. P. Grant, C. T. Johnson, E. P. Plummer, and F. Parpia, Comput. Phys. Commun. **55**, 425 (1989).
[64] MOLCAS version 3, K. Andersson, M. R. A. Blomberg, M. P. Fülscher, V. Kellö, R. Lindh, P.-Å. Malmqvist, J. Noga, J. Olsen, B. O. Roos, A. J. Sadlej, P. E. M. Siegbahn, M. Urban, and P.-O. Widmark, University of Lund, Sweden, 1994.
[65] M. Douglas and N. M. Kroll, Ann. Phys. **82**, 89 (1974).
[66] B. A. Hess, Phys. Rev. A **33**, 3742 (1986).
[67] M. Dolg (personal communication).
[68] K. P. Huber and G. Herzberg, *Constants of Diatomic Molecules* (van Nostrand Reinhold, New York, 1979).
[69] J. Teichteil, J. Chim. Phys. **87**, 963 (1990).
[70] J. B. Koffend, A. M. Sibai, and R. Bacis, J. Phys. **43**, 1639 (1981).
[71] S. Gestenkorn, P. Luc, and J. Vergès, J. Phys. B **14**, L193 (1981).
[72] T. Ishiwata, H. Ohtoshi, M. Sakaki, and I. Tanaka, J. Chem. Phys. **80**, 1411 (1984).
[73] P. M. Boerrigter, M. A. Buijse, and J. G. Snijders, Chem. Phys. **111**, 47 (1987).
[74] T. J. Lee and P. R. Taylor, Int. J. Quantum Chem. Symp. **23**, 199 (1989).